

RSDM-S: A Method for the Evaluation of the Shakedown Load of Elastoplastic Structures

Konstantinos V. Spiliopoulos and Konstantinos D. Panagiotou

Abstract To estimate the life of a structure, or a component, which are subjected to a cyclic loading history, the structural engineer must be able to provide safety margins. This is only possible by performing a shakedown analysis that belongs to the class of direct methods. Most of the existing numerical procedures addressing a shakedown analysis are based on the two theorems of plasticity and are formulated within the framework of mathematical programming. A different approach is presented herein. It is an iterative procedure and starts by converting the problem of loading margins to an equivalent loading of a prescribed time history. Inside an iteration, the recently published RSDM direct method is used, which assumes the decomposition of the residual stresses into Fourier series and evaluates its coefficients by iterations. It is proved that a descending sequence of loading factors is generated which converges, from above, to the shakedown load factor when only the constant term of the series remains. An elastic-perfectly plastic with a von Mises yield surface is currently assumed. The method may be implemented in any existing FE code and its efficiency is demonstrated by a couple of applications.

Keywords Direct methods · Shakedown analysis · RSDM

1 Introduction

High levels of cyclic loading are often applied on civil and mechanical engineering structures. The main source of such loadings on civil engineering structures, like bridges, pavements, buildings, offshore structures are heavy traffic, earthquakes or waves. Mechanical engineering structures, like nuclear reactors and aircraft gas turbine propulsion engines, also operate under high levels of cyclic mechanical and

K.V. Spiliopoulos (✉) · K.D. Panagiotou
Department of Civil Engineering, Institute of Structural Analysis and
Antiseismic Research, National Technical University of Athens,
Zografou Campus, Zografos, 157-80 Athens, Greece
e-mail: kvspilio@central.ntua.gr

K.D. Panagiotou
e-mail: kdpanag@central.ntua.gr

temperature loads. Under all these kinds of loadings, these structures are forced to develop plastic strains.

The question to assess the life cycle of a structure, or a structural component, so that it can safely carry the applied loads, is answered, mostly, on the basis of cumbersome time stepping calculations. To this end, one has to know the exact time history. A better alternative, that requires much less computing time, is offered by the direct methods that may predict whether, under the given loading, the structure will become unserviceable due to collapse or excessive inelastic deformations. In addition, if the complete time history of loading is not known, but only its variation intervals, direct methods are the only way to establish safety margins. Typical examples of direct methods are the limit and shakedown analyses.

One may prove that for structures whose material is stable [1] an asymptotic state exists [2]. Direct methods are numerical approaches that attempt to estimate this state right from the start of the calculations. The search for the elastic shakedown state is based, for small displacements and elastic-perfectly plastic structures, on either the lower bound [3] or the upper bound theorems [4].

Various extensions of the above theorems to the large displacement regime have appeared (e.g. [5]) or to elastic-perfectly plastic cracked bodies (e.g. [6]). The problems of different elasto-plastic behavior like linear (e.g. [7]) or non-linear kinematic hardening (e.g. [8]) have also been considered. Non associated plasticity behaviors have also been addressed (e.g. [9]). Shakedown theorems have also been written on the basis of gradient plasticity concepts [10].

As also mentioned above, the vast majority of the direct methods for the solution of the shakedown problem make use of either the lower or the upper bound theorems of plasticity. They are formulated within the framework of mathematical programming (MP) and aim to minimize or maximize an objective function. Depending on whether either the objective function or the constraints or both are linear or non-linear one has to solve a linear (e.g. [11]) or a nonlinear (e.g. [12]) programming problem.

Various techniques have been used to solve the MP program, among which one could mention the reduced basis technique (e.g. [13]). Since the advent of the interior point algorithms, which proved valuable to solve large scale optimization problems, many researchers have formulated, used and applied them to the shakedown analysis (e.g. [14–16]). Both the fields of solid and soil mechanics are referred to. More recent applications have recently appeared in [17].

The Linear Matching Method (LMM) [18] is one of very few alternative procedures to the MP methods. The approach is a generalization of the elastic compensation method [19] and is based on matching a linear problem to a plasticity problem. A sequence of linear solutions, with spatially varying moduli, is generated that provide upper bounds that monotonically converge to the least upper bound. The method has been widely applied to several steel structural components and recently to the limit analysis of concrete beams [20]. The method was further extended beyond shakedown, for loadings that can be decomposed into constant and time varying components, so as to provide an upper bound estimation of the ratchet boundary [21, e.g.], for a recent version.

A direct method to predict any long-term steady cycle of an elastic-perfectly plastic structure under a given cyclic loading was suggested recently [22]. The physics of the steady cycle, which assumes the cyclic nature of the residual stresses, is the main ingredient of the method. It has been called the Residual Stress Decomposition Method (RSDM) and is based on decomposing the residual stresses in Fourier series inside a cycle of loading.

The numerical procedure, presented herein, is a direct method for shakedown analysis [23]; it makes use of the RSDM, and is thus called RSDM-S. Since only the variation intervals are now known, the problem is converted to a prescribed loading problem by drawing a curve between these intervals. Starting from a load factor calculated so as to be above shakedown an iterative procedure is generated which is proved to converge to the shakedown load factor from above. Two examples of application are given. The whole approach is shown to be stable and computationally efficient, with uniform convergence.

2 Cyclic Elastoplastic States

A structure having volume V and surface S is subjected to cyclic surface tractions on one part and on the other part of S to zero displacements.

If the set of loads $\mathbf{P}(t)$ that act on S is a cyclic loading we may write:

$$\mathbf{P}(t) = \mathbf{P}(t + nT) \quad (1)$$

with t being a time point inside the cycle; T is the period of the cycle, $n = 1, 2, \dots$, denotes the number of full cycles. Bold letters are used, herein, to denote vectors and matrices.

Let us suppose that the structure is made of an elastic-perfectly plastic material. Let us further suppose that our structure has been discretized to finite elements and the stresses and strains refer to the Gauss points (GP).

The structure will develop, at a time point $\tau = t/T$ inside the cycle, a stress field $\boldsymbol{\sigma}(\tau)$, which may be decomposed into an elastic part $\boldsymbol{\sigma}^{\text{el}}(\tau)$, that equilibrates the external loading $\mathbf{P}(\tau)$, assuming a completely elastic behavior, and a self-equilibrating residual stress part $\boldsymbol{\rho}(\tau)$ that is due to inelasticity. Therefore:

$$\boldsymbol{\sigma}(\tau) = \boldsymbol{\sigma}^{\text{el}}(\tau) + \boldsymbol{\rho}(\tau) \quad (2)$$

The strain rates can also be decomposed analogously:

$$\dot{\boldsymbol{\epsilon}}(\tau) = \dot{\boldsymbol{\epsilon}}^{\text{el}}(\tau) + \dot{\boldsymbol{\epsilon}}_{\text{r}}(\tau) \quad (3)$$

The residual strain rate itself may be decomposed into an elastic and a plastic part [22]. Thus the final compatibility equation is expressed as:

$$\dot{\boldsymbol{\epsilon}}(\tau) = \dot{\boldsymbol{\epsilon}}^{\text{el}}(\tau) + \dot{\boldsymbol{\epsilon}}_{\text{r}}^{\text{el}}(\tau) + \dot{\boldsymbol{\epsilon}}^{\text{pl}}(\tau) \quad (4)$$

The elastic strain rates are related to the stress rates through the elasticity matrix \mathbf{D} , whereas the plastic strain rate vector $\dot{\mathbf{e}}^{\text{pl}}(\tau)$ through the gradient to the flow rule:

$$\begin{aligned}\dot{\boldsymbol{\sigma}}^{\text{el}}(\tau) &= \mathbf{D} \cdot \dot{\mathbf{e}} \\ \dot{\boldsymbol{\rho}}(\tau) &= \mathbf{D} \cdot \dot{\mathbf{e}}_r^{\text{el}} \\ \dot{\mathbf{e}}^{\text{pl}} &= \lambda \cdot \frac{\partial f}{\partial \boldsymbol{\sigma}}\end{aligned}\quad (5)$$

where f is the yield surface and $\boldsymbol{\sigma}$ is a stress state on the yield surface, i.e. $f(\boldsymbol{\sigma}) = 0$. A state of stress that lies either inside or on the yield surface, i.e. $f(\boldsymbol{\sigma}_*) \leq 0$, is an allowable stress state, whereas a state of stress $\boldsymbol{\sigma}_*$ that lies inside the yield surface, i.e. $f(\boldsymbol{\sigma}_*) < 0$, is a safe stress state.

As already mentioned in the introduction, for an elastoplastic material which is stable in the Drucker's sense [1], an asymptotic cyclic state always exists in which the stresses and strain rates stabilize and become periodic with the same period of the cyclic loading [2].

Depending on the amplitude of the load we may have unsafe conditions for the structure at hand, such as ratcheting or alternating plasticity, where we have asymptotically non vanishing plastic strain rates, or a safe long-term structural behavior, where, further plastic straining ceases to exist. This condition is the elastic shakedown.

The conditions for elastic shakedown to occur are given by Melan [3] which consists of two statements [24]:

- (a) The structure will shake down under a cyclic loading, if there exists a time-independent distribution of residual stresses $\bar{\boldsymbol{\rho}}$ such that, under any combination of loads inside prescribed limits, its superposition with the elastic stresses $\boldsymbol{\sigma}^{\text{el}}$, i.e. $\boldsymbol{\sigma}^{\text{el}} + \bar{\boldsymbol{\rho}}$, results to a safe stress state at any point of the structure,
- (b) Shakedown never takes place unless a time-independent distribution of residual stresses can be found such that under all the possible load combinations the sum of the residual and elastic stresses constitutes an allowable stress state.

These statements define the limit cycle for a structure subjected to a prescribed loading program. Parameters of this cycle are the shakedown load factor and the constant in time residual stress distribution which are unique and independent of the preceding deformation history [24].

It is these two parameters that the procedure RSDM-S presented underneath estimates. The method is based on the RSDM [22] which assumes the decomposition of the residual stresses of any cyclic elastoplastic state in Fourier series:

$$\boldsymbol{\rho}(\tau) = \frac{1}{2} \mathbf{a}_0 + \sum_{k=1}^{\infty} \{ \cos(2k\pi\tau) \cdot \mathbf{a}_k + \sin(2k\pi\tau) \cdot \mathbf{b}_k \} \quad (6)$$

with \mathbf{a}_0 , \mathbf{a}_k , and \mathbf{b}_k being the coefficients of the series found iteratively by the RSDM.

3 The Residual Stress Decomposition Method for Shakedown Analysis (RSDM-S)

The procedure is formulated for a maximum number of two loads P_1 and P_2 , although it may be applied for more than two loads. The loads are assumed to vary between a minimum value which for simplicity is assumed zero and a maximum value, which are denoted by P_1^* and P_2^* respectively.

We may use any curve that passes through these two limits to express a cyclic loading variation. The two loads may vary proportionally (Fig. 1a) or independently (Fig. 2a).

- (a) For proportional variation (Fig. 1)

The two loads in the time domain may be expressed by the following equation:

$$\mathbf{P}(\tau) = \begin{Bmatrix} P_1(\tau) \\ P_2(\tau) \end{Bmatrix} = \begin{Bmatrix} P_1^* \cdot \alpha(\tau) \\ P_2^* \cdot \alpha(\tau) \end{Bmatrix} \tag{7}$$

with $\alpha(\tau)$ being a time function common for both the loads. One possible smooth variation of a fourth order polynomial may be seen in Fig. 1c.

- (b) For independent load variation (Fig. 2)

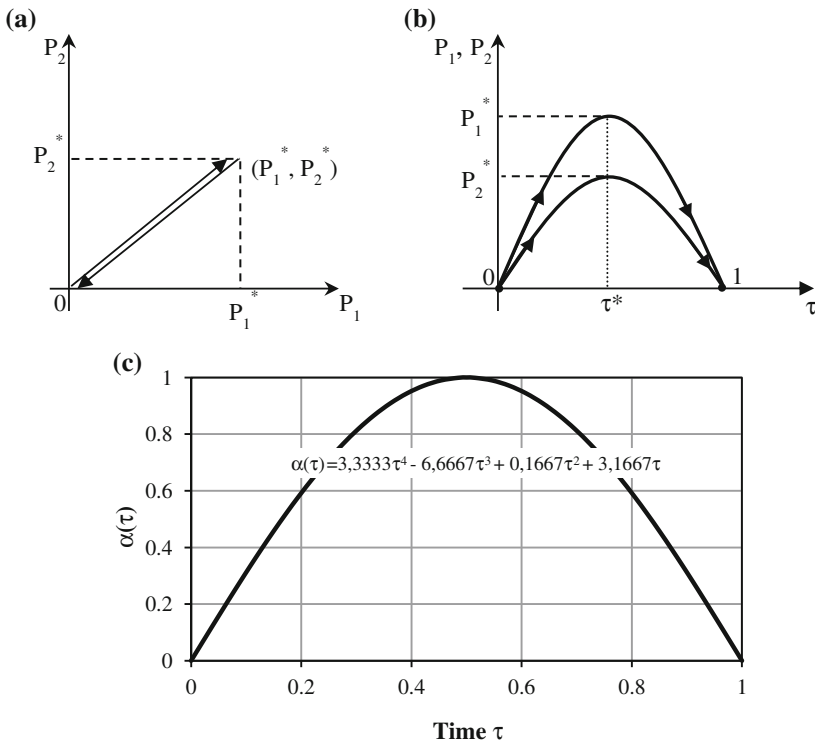


Fig. 1 Proportional loading variation a in load space, b in time domain c time function used

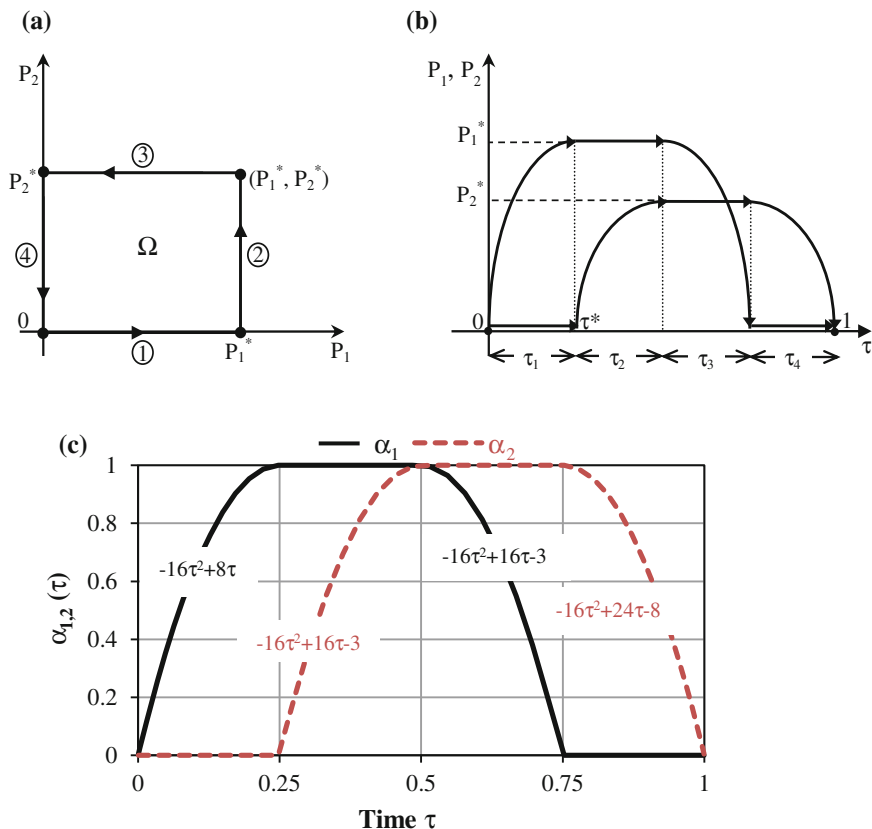


Fig. 2 Independent loading variation **a** in load space, **b** in time domain **c** time functions used

It has been proved in [25] that due to the convexity of the yield surface if a structure shakes down over the path that encloses the domain Ω , it certainly shakes down over any loading path contained inside this domain. This enclosing path may be described by the following equation:

$$\mathbf{P}(\tau) = \begin{Bmatrix} P_1(\tau) \\ P_2(\tau) \end{Bmatrix} = \begin{Bmatrix} P_1^* \cdot \alpha_1(\tau) \\ P_2^* \cdot \alpha_2(\tau) \end{Bmatrix} \quad (8)$$

Two time functions are used now (Fig. 2b) and a possible smooth variation is described in Fig. 2c, where a second degree polynomial is used for two quadrants of the cycle, whereas a constant non-zero and a zero value are employed inside the other two quadrants.

The load domains shown in Figs. 1 and 2 may be isotropically varied by multiplying them with a factor γ . Thus the numerical procedure is built, so that, starting from a load factor high above, this load factor is constantly lowered by shrinking the load domain in a continuous way up to the point that the shaken down load factor is reached.

The procedure is formulated herein for a von Mises yield surface. Although the procedure is general it will be formulated in the present work for two-dimensional structures of thickness d under plane stress conditions.

3.1 Initial Load Factor

From the way the loading time history is being constructed we may observe that when the loads vary proportionally (Fig. 1b, c), there always exists a cycle point τ^* that both the two loads attain their maximum values. On the other hand, for loads varying independently (Fig. 2b, c) the cycle point τ^* may be defined as the time point for which one of the two loads becomes maximum, with the other one being zero.

For either case, one may find the equivalent von Mises elastic stress $\bar{\sigma}^{\text{el}}$ at all the GPs of the structure at time τ^* . Denoting by $\min \bar{\sigma}^{\text{el}}$ the non-zero minimum of these stresses one may use an initial load factor equal to:

$$\gamma^{(0)} = \frac{\sigma_Y}{\min \bar{\sigma}^{\text{el}}} \quad (9)$$

where σ_Y is the yield stress of the material.

By choosing this load factor the starting conditions are definitely above the shakedown loading since the whole structure will have become plastic.

3.2 Development of the Procedure

Having found an initial solution, we use the RSDM [22] for the factored cyclic loading $\gamma^{(0)} \cdot \mathbf{P}(\tau)$, to produce an initial estimate for $\rho_{(0)}$, $\mathbf{a}_0^{(0)}$, $\mathbf{a}_k^{(0)}$, $\mathbf{b}_k^{(0)}$. Then we enter the iterative phase, which consists of two iteration loops, one inside the other.

The following iterative steps are then followed:

1. Inside an iteration κ of the outer loop, starting with $\kappa = 1$, the following expression, which is the sum of the norms of the vectors of the coefficients of the trigonometric part of the Fourier series of the residual stresses, is found:

$$\varphi \left(\gamma^{(\kappa-1)} \right) = \sum_{k=1}^{\infty} \left\| \mathbf{a}_k^{(\kappa-1)} \right\| + \sum_{k=1}^{\infty} \left\| \mathbf{b}_k^{(\kappa-1)} \right\| \quad (10)$$

2. An update of the loading factor may be calculated:

$$\gamma^{(\kappa)} \cdot \mathbf{P}_1^* = \gamma^{(\kappa-1)} \cdot \mathbf{P}_1^* - \omega \cdot [\varphi \left(\gamma^{(\kappa-1)} \right) \cdot d] \quad (11)$$

The expression (11) actually monitors the level of the applied loads with the reminder that d is the thickness of the structure. The update of the loading factor

is chosen to be performed in conjunction with the maximum of the two peaks of the applied loads, although any other time point could be used.

It should also be noted that ω is a convergence parameter, which will be discussed below.

3. The following inequality is checked:

$$\frac{|\gamma^{(k)} - \gamma^{(k-1)}|}{\gamma^{(k)}} \leq \text{tol} \quad (12)$$

4. If Eq. (12) holds, the procedure stops and $\gamma^{(k)} = \gamma^{(k-1)} = \gamma_{\text{sh}}$, otherwise we set

$$\boldsymbol{\rho}_{(k-1)}^{(1)}(\tau) = \boldsymbol{\rho}_{(k-1)}(\tau) \quad (13)$$

Using the updated load factor of the outer loop, an inner loop of iterations controlled by μ starts with $\mu = 1$. The steps of this inner loop are virtually the same steps with the RSDM [22].

5. The following expression is computed for each cycle point τ and for each GP:

$$\boldsymbol{\sigma}^{(\mu)}(\tau) = \gamma^{(k)} \boldsymbol{\sigma}^{\text{el}}(\tau) + \boldsymbol{\rho}_{(k-1)}^{(\mu)}(\tau) \quad (14)$$

where:

$$\boldsymbol{\sigma}^{\text{el}}(\tau) = \alpha_1(\tau) \boldsymbol{\sigma}_{\text{P}_1^*}^{\text{el}} + \alpha_2(\tau) \boldsymbol{\sigma}_{\text{P}_2^*}^{\text{el}} \quad (15)$$

with $\alpha_1(\tau)$, $\alpha_2(\tau)$ being the time functions for independent loading (Fig. 2b, c), whereas $\alpha_1(\tau) = \alpha_2(\tau) = \alpha(\tau)$ is the time function for the proportional loading case (Fig. 1b, c).

6. It is checked whether the total effective stress $\bar{\sigma}^{(\mu)}(\tau) > \sigma_Y$; if this does not hold we set $\xi = 0$, otherwise:

$$\xi = \frac{\bar{\sigma}^{(\mu)}(\tau) - \sigma_Y}{\bar{\sigma}^{(\mu)}(\tau)} \Rightarrow \boldsymbol{\sigma}_{\text{pl}}^{(\mu)}(\tau) = \xi \cdot \boldsymbol{\sigma}^{(\mu)}(\tau) \quad (16)$$

This operation is a radial return [26] type rule and may be graphically seen in Fig. 3. For a more detailed discussion the reader is referred to [22].

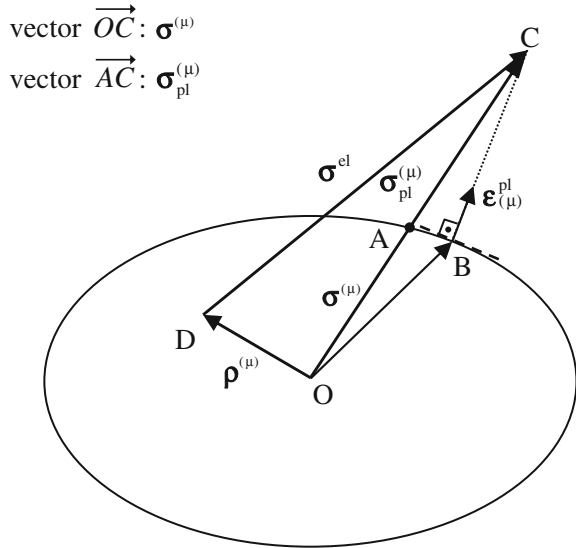
Steps 5 and 6 are repeated for every GP.

7. Assemble for the whole structure the new rate vector of the nodal forces $\dot{\mathbf{R}}'(\tau)$:

$$\dot{\mathbf{R}}'(\tau) = \gamma^{(k)} \dot{\mathbf{R}}(\tau) + \int_V \mathbf{B}^T \cdot \boldsymbol{\sigma}_{\text{pl}}^{(\mu)}(\tau) dV \quad (17)$$

with $\dot{\mathbf{R}}(\tau)$ being the equivalent nodal forces for the loading $\dot{\mathbf{P}}(\tau)$ which may be evaluated by differentiating the Eqs. (7) or (8), depending on the case of loading. \mathbf{B} is the compatibility strain-displacement matrix for the given FE mesh.

Fig. 3 Estimation of the plastic straining inside an iteration



8. We find an update for $\dot{\mathbf{r}}^{(\mu)}(\tau)$ using the relation

$$\mathbf{K}\dot{\mathbf{r}}^{(\mu)}(\tau) = \dot{\mathbf{R}}'(\tau) \tag{18}$$

with $\mathbf{K} = \int_V \mathbf{B}^T \mathbf{D} \mathbf{B} dV$ the structure's stiffness matrix.

9. A value for $\dot{\rho}^{(\mu)}(\tau)$ is evaluated at each G.P.

$$\dot{\rho}^{(\mu)}(\tau) = \mathbf{D} \mathbf{B} \dot{\mathbf{r}}^{(\mu)}(\tau) - \gamma^{(k)} \dot{\boldsymbol{\sigma}}^{\text{el}}(\tau) - \boldsymbol{\sigma}_{\text{pl}}^{(\mu)}(\tau) \tag{19}$$

where $\dot{\boldsymbol{\sigma}}^{\text{el}}(\tau) = \dot{\alpha}_1(\tau) \boldsymbol{\sigma}_{\text{p}_1^*}^{\text{el}} + \dot{\alpha}_2(\tau) \boldsymbol{\sigma}_{\text{p}_2^*}^{\text{el}}$

The steps 5–9 are repeated for all the cycle time points.

10. By performing numerical time integration over the whole cycle we may obtain an update of the Fourier coefficients [22]:

$$\begin{aligned} \mathbf{a}_k^{(\mu+1)} &= -\frac{1}{k\pi} \int_0^1 \left\{ \left[\dot{\rho}^{(\mu)}(\tau) \right] (\sin 2k\pi\tau) \right\} d\tau \\ \mathbf{b}_k^{(\mu+1)} &= \frac{1}{k\pi} \int_0^1 \left\{ \left[\dot{\rho}^{(\mu)}(\tau) \right] (\cos 2k\pi\tau) \right\} d\tau \\ \frac{\mathbf{a}_0^{(\mu+1)}}{2} &= -\sum_{k=1}^{\infty} \mathbf{a}_k^{(\mu+1)} + \frac{\mathbf{a}_0^{(\mu)}}{2} + \sum_{k=1}^{\infty} \mathbf{a}_k^{(\mu)} + \int_0^1 \left[\dot{\rho}^{(\mu)}(\tau) \right] d\tau \end{aligned} \tag{20}$$

11. From these updates one may get an update for $\boldsymbol{\rho}^{(\mu+1)}(\tau)$ using the iterative form of (6):

$$\boldsymbol{\rho}^{(\mu+1)}(\tau) = \frac{1}{2} \mathbf{a}_0^{(\mu+1)} + \sum_{k=1}^{\infty} \left\{ \cos(2k\pi\tau) \cdot \mathbf{a}_k^{(\mu+1)} + \sin(2k\pi\tau) \cdot \mathbf{b}_k^{(\mu+1)} \right\} \quad (21)$$

12. Next we check whether the values of the residual stresses at the current and at the previous iteration differ within some tolerance at some cycle point [22], for example at the end of the cycle, where $\tau = t/T = 1$, i.e.:

$$\frac{\|\boldsymbol{\rho}^{(\mu+1)}(1)\| - \|\boldsymbol{\rho}^{(\mu)}(1)\|}{\|\boldsymbol{\rho}^{(\mu+1)}(1)\|} \leq \text{tolr} \quad (22)$$

In case this does not hold we set $\boldsymbol{\rho}_{(\kappa-1)}^{(\mu+1)}(\tau) = \boldsymbol{\rho}^{(\mu+1)}(\tau)$ and go back to step 5 and start a new iteration of the inner RSDM loop; otherwise we set $\boldsymbol{\rho}_{(\kappa)}(\tau) = \boldsymbol{\rho}^{(\mu+1)}(\tau)$ and go back to step 1 and start a new iteration of the outer loop with $\kappa = \kappa + 1$.

For accurate results, the values 10^{-4} – 10^{-5} of *tolr* and 10^{-4} for *tol* are sufficient. The corresponding tolerance value for the function of φ (Eq. (10)) is 10^{-3} .

Due to the positive nature of φ , the algorithm generates a descending sequence of cyclic solutions which ends up with the parameters of the limiting cycle for elastic shakedown. Thus γ_{sh} is the elastic shakedown factor, and the constant term, which is the only remaining term in the Fourier series, is the constant in time distribution of the residual stresses, unique [24] for the adopted prescribed loading program.

3.3 Numerical Strategy

The numerical strategy adopted is to start the procedure with the convergence parameter $\omega = 1$. This normally leads to a monotonic convergence, from above, to the shakedown load. There could be cases, though, especially when we start from a high initial value that an overshooting of the shakedown factor occurs. In such a case, for the loading factor evaluated at the current iteration $\gamma^{(\kappa)}$, we would have $\varphi(\gamma^{(\kappa)}) < 10^{-3}$; this loading factor is then not accepted and the convergence factor is halved till we get a loading factor $\varphi(\gamma^{(\kappa)}) > 10^{-3}$ [23].

4 Application Examples

The method is applied to two examples of plated structures, a holed square plate under biaxial load and a grooved plate under tension and bending. Plane stress conditions are assumed.

4.1 Plate with a Central Hole

A square plate having a central hole is treated as a first example of application. The plate is subjected to two uniformly distributed loads acting at the two edges of the plate (Fig. 4). Due to the symmetry of the structure and the loading only a quarter of the plate is analyzed.

As far as the geometric characteristics of the plate, the ratio of the diameter D to the length L of the hole was considered equal to 0.2; the ratio of the thickness d of the plate to its length is taken 0.05. The case of a length $L = 20$ cm was used.

The finite element mesh is also shown in Fig. 4. Ninety-eight, eight-noded, isoparametric elements with 3×3 Gauss integration points were used.

The material data considered are Young's modulus $E = 210$ Gpa, Poisson's ratio $\nu = 0.3$ and yield stress $\sigma_Y = 360$ Mpa.

Both cases of proportional and independent variations of loads are presented. The shakedown loads for different ratios of the maximum values of the applied loads are given in Figs. 5 and 6.

For the proportional loading case the time function of Fig. 1c is used. One may see a good agreement with corresponding results (Fig. 5), reported in the literature [27].

For the independent load variation (Fig. 2), the time functions, whose equations for each part of the cycle, shown in Fig. 2c, are used. One may see good agreement (Fig. 6) with reported in the literature results that are based either on the LMM [27] or a mathematical programming algorithm [28]. The better agreement with [28] is due to the fact that a similar finite element mesh is constructed with the one used here.

One may realize the smoothness of the convergence of the method in Fig. 7 where the case of $P_1^* = P_2^*$ is shown. Analogous curves are obtained for all the other ratios.

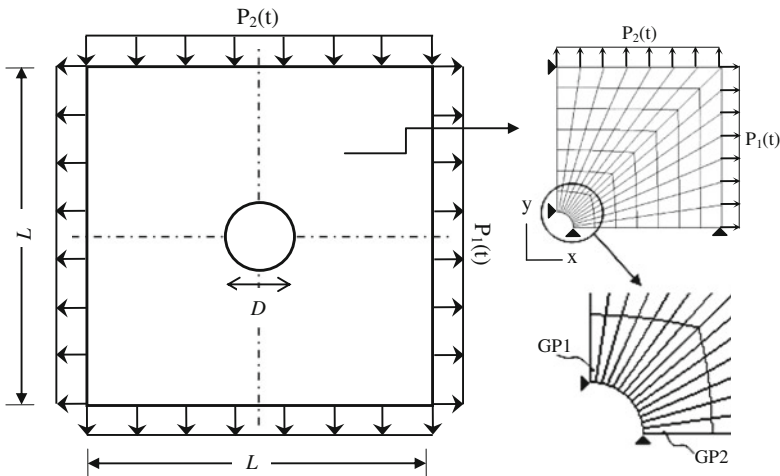


Fig. 4 Geometry, loading and FE discretization of the plate

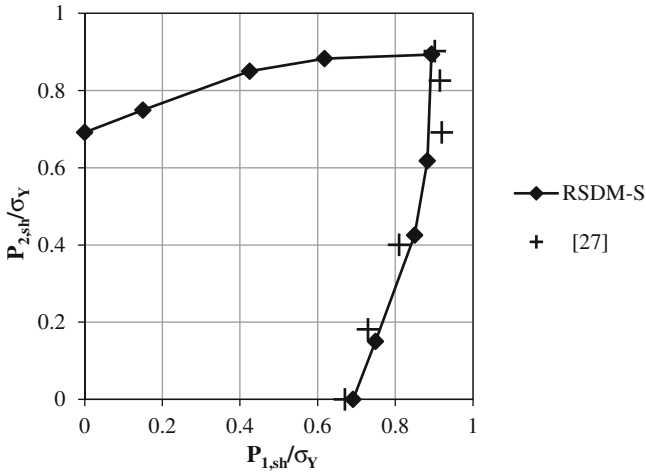


Fig. 5 Shakedown domain for the case of proportional loading

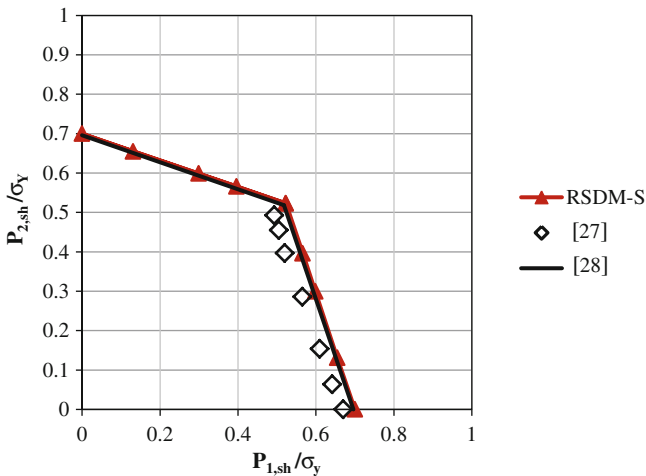


Fig. 6 Shakedown domain for the case of independent loading

Only the initial value of $\omega = 1$ was needed for convergence. In Fig. 8 one may also see a typical evolution of the plastic stress to zero at one of most stressed GPs, that are located at the two corners of the hole of the plate (Fig. 4). The CPU time reported to reach a solution for an Intel Core i7 at 2.93 GHz with 4,096 MB RAM was of the order of 40 s.

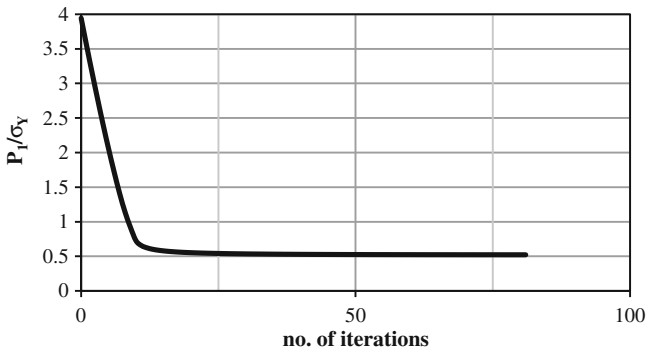


Fig. 7 Convergence of the RSDM-S for the holed plate, for equal maximum loads

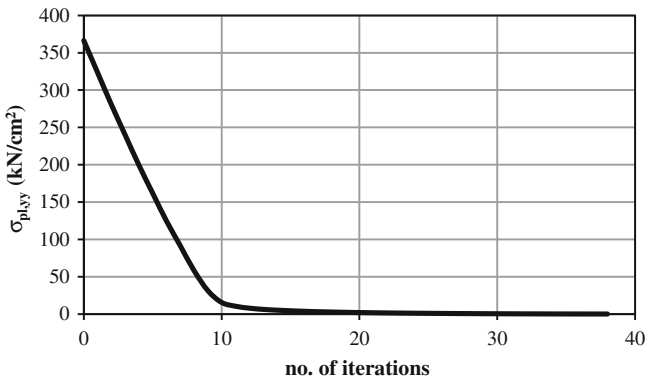


Fig. 8 Evolution of the yy component of the plastic stress vector at GP2 at the 3T/4

4.2 Grooved Rectangular Plate Under Varying Tension and Bending

The second example of application deals with a grooved rectangular plate subjected to an in plane constant tension $P_N(t)$ and a linearly varying bending moment $P_M(t)$ along the boundaries (Fig.9). A rectangular loading domain is considered (Fig.2) with the two loads varying independently, having maximum values $P_N^* = 1$ and $P_M^* = 1$, respectively. This example has been presented in [29].

The following geometrical data are used: $R = 25$ cm, $L = 2R$ and $H = 4R$.

The plate is assumed homogeneous, isotropic, elastic-perfectly plastic with the following material data: Young’s modulus $E = 210$ GPa, Poisson’s ratio $\nu = 0.3$ and yield stress $\sigma_Y = 111.62$ MPa.

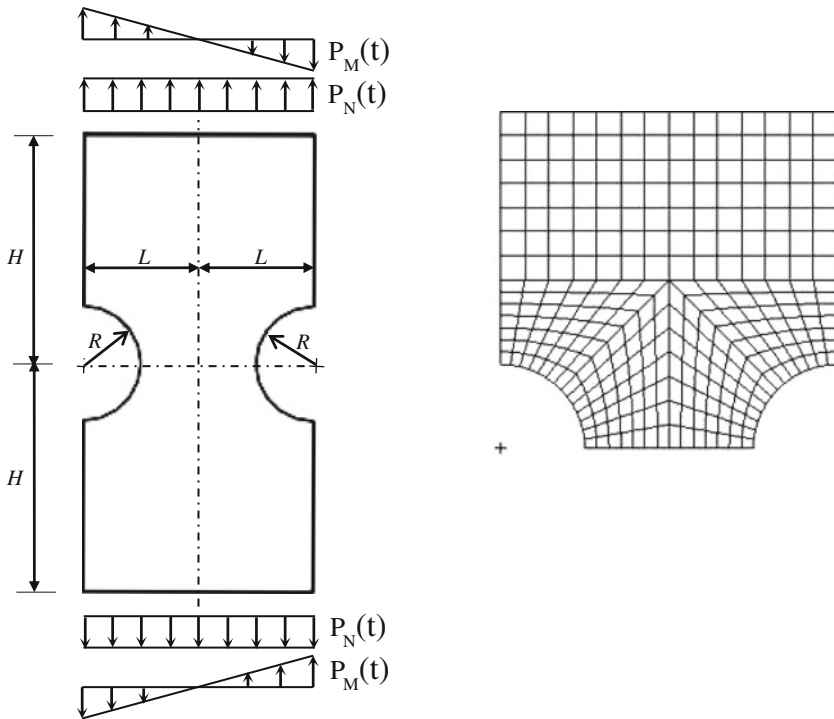


Fig. 9 Geometry, loading of the grooved rectangular plate and its finite element mesh

Due to the symmetry of the geometry and the applied loads, only a half of the structure has been modeled. The finite element mesh discretization of the plate is also shown in Fig. 9. Two hundred and ninety-four, eight-noded, iso-parametric elements with 3×3 Gauss integration points were used.

The shakedown domain obtained by the RSDM-S and its comparison with the results from [29] is shown in Fig. 10.

Specifically in the case we have both in-plane tension and bending with $P_N^* = P_M^*$ the proposed RSDM-S gives a shakedown factor equal to 0.227 which quite close to the value 0.236 of [29], where a different mesh and algorithm was used.

For this example, the initial convergence parameter $\omega = 1$, in the process of the iterations, had to be halved twice, due to an overshooting of the calculated shakedown load to negative values.

Although the starting point was quite high as compared to the final result, the descent was rapid as shown in the Fig. 11. In the insert of the figure, one may see, after the initial descent, the smooth convergence towards the shakedown value.

In this example the CPU time reported to reach the solution for a CPU with the same characteristics as above was of the order of 270 s.

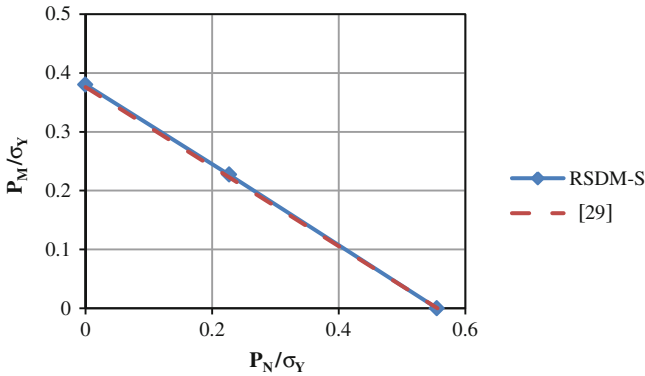


Fig. 10 Shakedown domain of the grooved rectangular plate in tension and bending

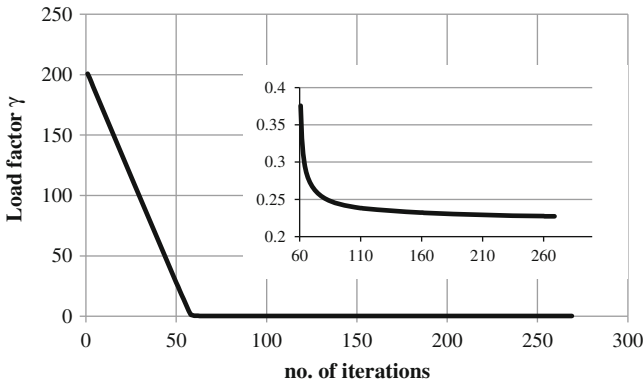


Fig. 11 Convergence of the RSDM-S towards the shakedown factor for the grooved rectangular plate

5 Concluding Remarks

A novel direct method to calculate the shakedown load of structures exhibiting elasto-plastic material behavior when subjected to cyclic loadings has been introduced.

The procedure is iterative in its nature and starts by converting a loading of prescribed limits to a loading of a prescribed cyclic history. This history is then multiplied by a factor. A sequence of decreasing factors, whose initial value is calculated to be above the shakedown load, is generated by the method. For each factored cyclic loading history the distribution of the residual stresses of the corresponding cyclic elasto-plastic state is estimated. This is done by decomposing these stresses into Fourier series and finding their coefficients also iteratively. The procedure stops when only the constant term of the series remains. Thus the method converges to the shakedown load factor from above.

It is a relatively simple method, formulated within the FE method. The stiffness matrix of the structure needs to be formed and decomposed only once. Three terms of the Fourier series are enough for accurate results. These two factors guarantee the method to be numerically efficient.

The main advantage of the method is that the solution procedure provides a better understanding of the physics of the problem than any method based on MP algorithms. At the same time, the absence of such an algorithm makes it directly implementable into any existing FE software.

Although the method has been applied here to two-dimensional structures, three-dimensional structures can be also considered. It may also be extended to loading domains of more than two loads. Other yield surfaces, except for von Mises, may be considered. Also, besides perfect plasticity, other plasticity laws, like strain hardening, may be taken care of.

References

1. Drucker DC (1959) A definition of stable inelastic material. *ASME J Appl Mech* 26:101–106
2. Frederick CO, Armstrong PJ (1966) Convergent internal stresses and steady cyclic states of stress. *J Strain Anal* 1:154–169
3. Melan E (1938) Zur Plastizität des räumlichen Kontinuums. *Ing Arch* 9:116–126
4. Koiter W (1960) General theorems for elastic-plastic solids. In: Sneddon IN, Hill R (eds) North-Holland, Amsterdam
5. Weichert D (1986) On the influence of geometrical nonlinearities on the shakedown of elastic-plastic structures. *Int J Plast* 2:135–148
6. Belouchrani MA, Weichert D (1999) An extension of the static shakedown theorem to inelastic cracked structures. *Int J Mech Sci* 41:163–177
7. Pham DC (2005) Shakedown static and kinematic theorems for elastic-plastic limited linear kinematic hardening solids. *Eur J Mech A/Solids* 24:35–45
8. Simon J-W (2013) Direct evaluation of the limit states of engineering structures exhibiting limited, nonlinear kinematical hardening. *Int J Plast* 42:141–167
9. Bousshine L, Chaaba A, de Saxcé G (2003) A new approach to shakedown analysis for non-standard elastoplastic material by the bipotential. *Int J Plast* 19:583–598
10. Polizzotto C (2008) Shakedown theorems for elastic-plastic solids in the framework of gradient plasticity. *Int J Plast* 24:218–241
11. Maier G (1969) Shakedown theory in perfect elastoplasticity with associated and nonassociated flow-laws: a finite element, linear programming approach. *Meccanica* 4:1–11
12. Stein E, Zhang G, König JA (1992) Shakedown with nonlinear strain-hardening including structural computation using finite element method. *Int J Plast* 8:1–31
13. Heitzer M, Staat M (2003) Basis reduction technique for limit and shakedown problems. In: Staat M, Heitzer M (eds) Numerical methods for limit and shakedown analysis. NIC Series, vol 15, pp 1–55
14. Andersen KD, Christiansen E, Overton ML (1998) Computing limit loads by minimizing a sum of norms. *SIAM J Sci Comput* 19:1046–1062
15. Vu DK, Yan AM, Nguyen-Dang H (2004) A primal-dual algorithm for shakedown analysis of structures. *Comput Methods Appl Mech Eng* 193:4663–4674
16. Simon J-W, Höer D, Weichert D (2014) A starting-point strategy for interior-point algorithms for shakedown analysis of engineering structures. *Eng Optim* 46(5):648–668
17. Spiliopoulos K, Weichert D (2014) Direct methods for limit states in structures and materials. Springer, Berlin

18. Ponter ARS, Carter KF (1997) Shakedown state simulation techniques based on linear elastic solutions. *Comput Methods Appl Mech Eng* 140:259–279
19. Mackenzie D, Boyle T (1993) A method of estimating limit loads by iterative elastic analysis. I—Simple examples. *Int J Press Vessel Pip* 53:77–95
20. Pisano AA, Fuschi P, de Domenico D (2013) A kinematic approach for peak load evaluation of concrete elements. *Comput Struct* 119:125–139
21. Chen H, Ponter ARS (2010) A direct method on the evaluation of ratchet limit. *ASME J Press Vessel Technol* 132(4):1–8
22. Spiliopoulos KV, Panagiotou KD (2012) A direct method to predict cyclic steady states of elastoplastic structures. *Comput Methods Appl Mech Eng* 223–224:186–198
23. Spiliopoulos KV, Panagiotou KD (2014) A residual stress decomposition based method for the shakedown analysis of structures. *Comput Methods Appl Mech Eng* 276:410–430
24. Gokhfeld DA, Cherniavsky OF (1980) Limit analysis of structures at thermal cycling. Sijthoff & Noordhoff, Alphen aan den Rijn
25. König JA, Kleiber M (1978) On a new method of shakedown analysis. *Bull Acad Polon Sci Ser Sci Tech* 26:165–171
26. Simo JC, Hughes TJR (1998) *Computational inelasticity*. Springer, New York
27. Ponter ARS, Engelhardt M (2000) Shakedown limits for a general yield condition: implementation and application for a von Mises yield condition. *Eur J Mech A/Solids* 19:423–445
28. Carvelli V, Cen ZZ, Liu Y, Maier G (1999) Shakedown analysis of defective pressure vessels by a kinematic approach. *Arch Appl Mech* 69:751–764
29. Tran TN, Liu GR, Nguyen XH, Nguyen TT (2010) An edge-based smoothed finite element method for primal-dual shakedown analysis of structures. *Int J Numer Eng* 82:917–938